Equivalent Broadband Electrical Circuit of Synchronous Machine Winding for Frequency Response Analysis Based on Gray Box Model

Zhongyong Zhao, *Member, IEEE*, Yu Chen, Yueqiang Yu, Mengyuan Han, Chao Tang, *Member, IEEE*, and Chenguo Yao, *Member, IEEE*

***Abstract*—Frequency response analysis (FRA) is a popular tool to detect transformer winding deformation faults. It has been recently used to diagnose the winding inter-turn short circuit fault of the electric machine. The application of FRA is based on the fact that the winding can be equivalent to an electrical circuit consisting of resistance, inductance, and capacitance. Therefore, to obtain an accurate broadband equivalent circuit model of synchronous machine and perform the fault analysis and diagnosis, this paper introduces the gray box model technique based on the state space and genetic algorithm. The electrical circuit of a form-wound coil of a 4 kW machine with known electrical parameters is used to verify the proposed method primarily. Besides, the equivalent circuit modeling is carried out and experimentally verified on an actual 5 kW synchronous machine. Finally, the fault simulation analyses of winding inter-turn short circuits are performed based on the proposed equivalent electrical circuit. The verification result shows that the circuit parameters identified by the proposed method are accurate. Moreover, the fault simulation results indicate that the inter-turn short circuit faults can cause apparent variations in the frequency response curves. It is feasible to detect the winding fault of the synchronous machine by the FRA method.**

***Index Terms*—Synchronous machine, winding, inter-turn short circuit, frequency response, equivalent electrical circuit, state space.**

I. Introduction

ELECTRIC machinery is an energy conversion device that can transform or transfer electric energy and mechanical energy, which has been widely used in industry [1]. In all kinds of power generation methods, 90% of the power is supplied by the synchronous machine. The synchronous machines have to withstand thermal stress, electromagnetic stress, mechanical stress, electromagnetic noise, vibration, the rotor's centrifugal force, aging of the insulation material, and other faults in the operations, which may induce severe defects of the machines. Synchronous machine faults can be generally divided into gear and bearing faults, stator and rotor faults [2]. Among them, short-circuit fault of the stator winding is a typical fault, which has a certain probability of occurrence, but serious consequences [3]. The inter-turn short circuit fault between stator windings may cause changes in electromagnetic force distribution, distortion of the voltage waveform, excessive winding temperature, and increased vibration. These defects may further induce one-point grounding faults and other more severe faults. Therefore, the accurate detection of the stator winding inter-turn short circuit and other spots is significant to the synchronous machine's reliable operation.

Nowadays, the primary methods to detect short-circuit faults of synchronous machine windings include DC resistance measurement method, AC impedance/dielectric dissipation method [4], recurrent surge oscilloscope (RSO) method [5], open-end transformer method, detection coil method, and traveling wave method [6]. However, the DC resistance measurement method is more effective when the number of short-circuit turns is large. The AC impedance/dielectric dissipation method has higher sensitivity, but its detection effect can be affected by the impedance and residual magnetism of the rotor and stator loss. For the RSO method, although it is sensitive, it cannot locate the short circuit point of the winding. The open-end transformer method is affected by the rotor slot wedge material and the tightness between slot wedge and slot wall; the rotor should be pulled out before the test.

Some researchers have proposed using frequency response analysis (FRA) to detect the synchronous machine's short circuit faults [7]–[10]. FRA is a popular and powerful tool to detect transformer winding mechanical deformation faults. The FRA measurement can include four connection modes: end-to-end open circuit, end-to-end short circuit, inductive coupling, and capacitive coupling. FRA has the advantages of high sensitivity, fast diagnosis, economic and non-destructive procedure [11]–[14]. Its basic principle is that the winding can be equivalent to

Manuscript received February 1, 2021; revised April 11, 2021; accepted May 15, 2021. Date of publication May 19, 2021; date of current version November 23, 2021. This work was supported in part by the National Natural Science Foundation of China under Grant 51807166, by the Natural Science Foundation of Chongqing under Grant cstc2019jcyj-msxmX0236, and by the Venture and Innovation Support Program for Chongqing Overseas Returnees under Grant cx2019123. *(Corresponding author: Zhongyong Zhao.)*

Zhongyong Zhao, Yu Chen, Yueqiang Yu, Mengyuan Han, and Chao Tang are with the College of Engineering and Technology, Southwest University, Chongqing 400716, China (e-mail: zhaozy1988@swu.edu.cn; cy1034429543@email.swu.edu.cn; yuyueqiang@swu.edu.cn; hanmengyuan@swu.edu.cn; tangchao_1981@163.com).

Chenguo Yao is with the State Key Laboratory of Power Transmission Equipment and System Security and New Technology, Chongqing University, Chongqing 400044, China (e-mail: yaochenguo@cqu.edu.cn).

Color versions of one or more figures in this article are available at https://doi.org/10.1109/TEC.2021.3081933.

Digital Object Identifier 10.1109/TEC.2021.3081933

a broadband equivalent circuit model consisting of capacitance, resistance, and inductance in the high-frequency range. The occurrence of winding short circuit, mechanical deformation, or displacement faults will inevitably cause the variations in the structure or parameters of equivalent circuit model, resulting in a change in the frequency response characteristics of the winding, thus, from which the failure state of the winding can be diagnosed [15]–[16]. Therefore, an accurate broadband equivalent circuit model of winding is the basis for the fault analysis of the synchronous machine using the FRA method.

Currently, the equivalent modeling methods of synchronous machine windings can be divided into the following categories. One is to model the winding based on its structural and geometric parameters, called the white-box model. A high-frequency phase variable model for PM synchronous motor is proposed based on the finite element-circuit coupling analysis [17]. The basic unit in the model represents the individual winding turn. After the original model is obtained by solving the equivalent inductance and capacitance with the magnetostatic and electrostatic field solver, the Kron matrix reduction technology is applied to the distributed-parameter winding circuit to get a lumped high-frequency branch. The final model is used for electromagnetic interference (EMI) prediction. Reference [18] calculates the equivalent capacitance, inductance, and resistance of winding by empirical formula method and establishes the equivalent lumped parameter broadband electrical model.

Another modeling idea mathematically fits the impedance amplitude-frequency characteristics measured at the machine's terminal based on the simple resonant circuit. The established model is called the black-box model. Reference [19] presents a fast modeling method for the synchronous machine's broadband equivalent circuit model in electric vehicles (EV). The measured broadband impedance curve is divided into several regions based on the resonance point, an RLC resonant unit is used to simulate each region, and all units are cascaded. Reference [20] measures the wideband impedance characteristics of a synchronous machine in common and differential mode. The asymptotic and empirical formula method is used to solve the equivalent circuit parameters. The established equivalent circuit model is used to predict the time and frequency domain characteristics of electric machinery in the EMI frequency band from 10 kHz to 30 MHz.

However, there exist imperfections in the above two methods.

1) The structure, dimensions and material parameters of windings and cores need to be known beforehand when using the white-box model, whether it is the finite element method or the empirical formula method. For small and medium rated power electric machinery, the windings are mostly parallel enameled round wires, making the winding structure complex. Therefore, synchronous machines' modeling process using this method is challenging to achieve, and the results are not acceptable.
2) On the other hand, the model's terminal characteristics can be in good agreement with the measured one based on the solutions using the black-box model; however, some models are established by fitting method from a mathematic point of view. Besides, although windings' external characteristics can be appropriately characterized, the circuit parameters have no physical significance, making it unsuitable for assessing windings' internal status.

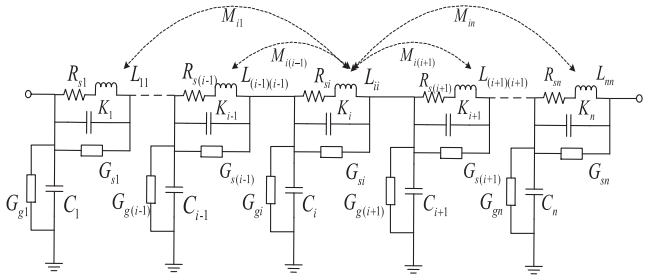

Fig. 1. Broadband equivalent electrical circuit of synchronous machine.

Therefore, this paper presents a method for modeling the equivalent broadband circuit of synchronous machine windings based on the gray-box model. The gray-box model is between the white-box model and the black-box model, which considers the equivalent parameters with physical meaning and the winding's external terminal characteristics. Compared with the approach followed in [20] and other methods, the proposed model is built based on automatic parameter extraction, it can also be used to simulate internal winding faults of the machine for frequency response analysis.

In this proposal, the state-space model is used to obtain the terminal broadband transfer function of the lumped parameter circuit of machine windings. Besides, the impedance or transfer function is combined with the actual measured terminal broadband characteristic. The intelligent genetic algorithm (GA) is used to identify the circuit model's equivalent parameters. Finally, the winding short circuit fault is also simulated, and the fault analysis is carried out.

II. Theory of Modeling Equivalent Circuit for Synchronous Machine Windings

A. The Transfer Function of Electric Machinery Winding Based on State-Space Model

Studies in references [8], [15], [18], [21] show that synchronous machine windings' electrical characteristics can be represented by a linear distributed parameter network composed of resistance, inductance, and capacitance in high-frequency ranges (1 kHz-30 MHz). The distributed circuit can be further equivalent to a lumped parameter circuit. In the circuit model, the inductance includes self-inductance of winding and mutual inductance between units. The capacitance includes capacitance between units and capacitance of winding to the core, as shown in Fig. 1. In Fig. 1, R_{si} and L_{ii} represent the resistance and leakage inductance of stator winding, K_i and G_{si} are capacitance and stray conductance between the adjacent units of windings out of stator slot. C_i and G_{gi} are stray capacitance and conductance of winding to the core. M_{in} is the mutual inductance between the *i*th inductance unit to the *n*th inductance unit. Because the stray conductance of the winding is relatively smaller than other parameters in practice, it can be ignored in the analysis.

For the node *i*, the Kirchhoff current law (*KCL*) and Kirchhoff voltage law (*KVL*) equations are listed and shown in (1) and (2):

$$V_i - V_{i+1} = R_{si} I_i + L_{ii} \dot{I}_i \sum_{k=1, k\neq i}^{n} M_{ik} \dot{I}_k \tag{1}$$

$$\begin{aligned} I_i - I_{i+1} = {} & K_i(\dot{V}_{i+1} - \dot{V}_i) + G_{si}(V_{i+1} - V_i) \\ & + G_{g(i+1)} V_{i+1} C_{i+1} \dot{V}_{i+1} + K_{i+1}(\dot{V}_{i+1} - \dot{V}_{i+2}) \\ & + G_{s(i+1)}(V_{i+1} - V_{i+2}) \end{aligned} \tag{2}$$

Where V_i is the voltage of C_i, I_i is the current of L_{ii}, and n is the order of the circuit.

When the state-space model is used to analyze the above circuit, the grounded capacitance's voltage and series inductance's current are selected as the state variables. Then the loop voltage and node current equations of (1) and (2) are written for the entire circuit, then the equations are written in matrix form:

$$HI = C\dot{V} + GV \tag{3}$$

$$TV = RI + L\dot{I} \tag{4}$$

Where H is the current coefficient matrix, T is the voltage coefficient matrix, R is the resistance matrix, L is the inductance matrix, C is the capacitance matrix, and G is the conductance matrix. The power supply voltage is selected as V_{in}, and V_{in} is extracted for calculating the terminal broadband characteristics (transfer function or impedance),

$$HI = C_0 \dot{V}_{in} + C_s \dot{V}_s + G_0 V_{in} + G_s V_s \tag{5}$$

$$T_0 V_{in} + T_s V_s = RI + L\dot{I} \tag{6}$$

Where T_0 is the first column matrix of T, T_s is the matrix of T with the first column removed, V_s is the matrix of V with V_{in} removed, G_0 is the first column of G, C_0 is the first column of C, G_s is the matrix of G with G_0 removed, C_s is the matrix of C with C_0 removed.

Transform the above formula to the following matrix form:

$$\begin{aligned} \begin{pmatrix} C_s & 0 \\ 0 & L \end{pmatrix} \begin{pmatrix} \dot{V}_s \\ \dot{I} \end{pmatrix} = {} & \begin{pmatrix} -G_s & H \\ T_s & -R \end{pmatrix} \begin{pmatrix} V_s \\ I \end{pmatrix} \\ & + \begin{pmatrix} -G_0 \\ T_0 \end{pmatrix} V_{in} + \begin{pmatrix} -C_0 \\ 0 \end{pmatrix} \dot{V}_{in} \end{aligned} \tag{7}$$

In the formula, $X = \binom{V_s}{I}$, $A = \left(\begin{smallmatrix} C_s & 0 \\ 0 & L \end{smallmatrix}\right)$, $P = \binom{-G_0}{T_0}$, $Q = \binom{-C_0}{0}$, $B = \left(\begin{smallmatrix} -G_s & H \\ T_s & -R \end{smallmatrix}\right)$,

$$A\dot{X} = BX + PV_{in} + Q\dot{V}_{in} \tag{8}$$

Both the voltage and current can be used as the output variable; the output equation is then as follows:

$$Y = MX \tag{9}$$

The Laplace transformations are used for (8) and (9), and the transfer function can be obtained by eliminating the state variable X:

$$H(s) = \frac{Y(s)}{V_{in}(s)} = M(sA - B)^{-1}(P + sQ) \tag{10}$$

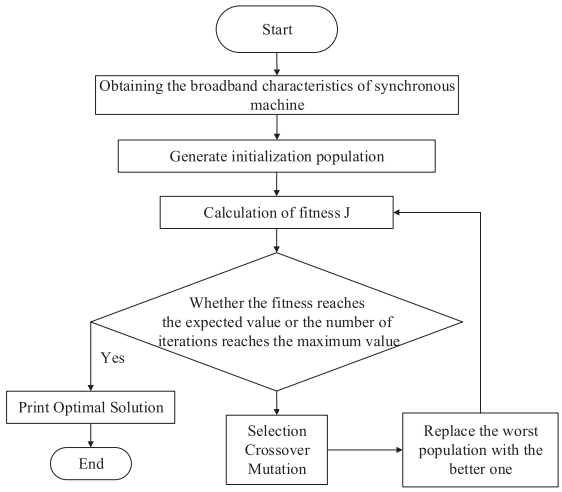

Fig. 2. Flow chart of optimizing equivalent electrical parameters of synchronous machine by genetic algorithm.

B. Fundamentals of FRA

The FRA technique is based on appliying a sinuous input voltage ($V_{\rm in}$) with variable frequency to one terminal of winding. The output voltage ($V_{\rm out}$) is measured at the other free terminal by a shunt impedance of 50 Ω. The FRA curve's amplitude-frequency characteristic is obtained using (11), which is commonly presented in dB units, while the phase-frequency characteristic is obtained using (12).

$$H_{dB} = 20\log_{10} \left| \frac{\vec{V}_{out}}{\vec{V}_{in}} \right| \tag{11}$$

$$\phi_0 = \frac{180}{\pi} \arg \left| \frac{\vec{V}_{out}}{\vec{V}_{in}} \right| \tag{12}$$

The commercial FRA analyzer generates a sinusoidal voltage signal of 20 V_{pp}, whose frequency ranges from 10 Hz to 2 MHz.

C. Fundamentals and Flow Chart of Genetic Algorithm

In this study, GA is used to optimize and identify the broadband equivalent circuit model parameters of the synchronous machine. In GA, selection, crossover, and mutation are three critical steps of genetic operations. The initial populations are produced by binary coding, and new individuals are created by mating the individuals through genetic operations. Parts of individuals are eliminated according to the principle of survival of the fittest until an optimal individual is selected, which would be the solution of the optimization problem [16]. The flow chart of optimizing equivalent electrical parameters of the synchronous machine by the genetic algorithm is shown in Fig. 2.

Fitness function: to calculate the broadband equivalent circuit parameters of synchronous machine by GA, the terminal broadband characteristics (impedance or transfer function) of the machine need to be measured, and the following fitness function

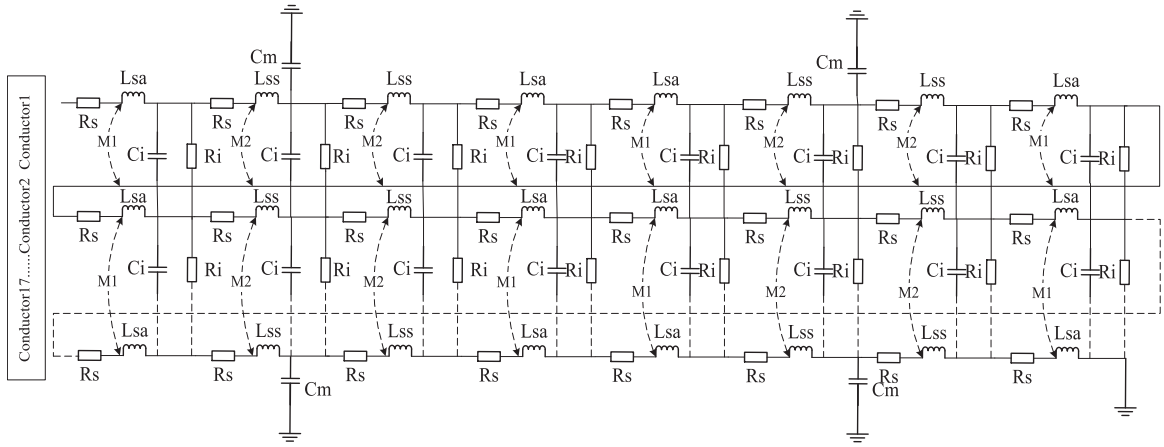

Fig. 3. Equivalent lumped parameter circuit for a stator coil of 4 kW machine [18].

J is constructed:

$$J = \sum_{f=1}^{N} \left(\frac{H_m(f) - H_d(f)}{H_m(f)} \right)^2 \tag{13}$$

Where H_{m} is the measured terminal broadband characteristic of electric machinery. H_{d} is the calculated terminal broadband characteristic based on state-space model shown in (10), *f* is the frequency point, and *N* is the number of data points.

III. Simulation Verification of Proposed Method Based on an Equivalent Circuit of Stator Coil of Machine

A. Introduction of Simulated Equivalent Circuit

The equivalent circuit of a 4 kW AC machine's stator coil is introduced in [18]. A form-wound stator coil has 17 turns per slot. The equivalent lumped parameter circuit is established based on the helical structure. In the circuit, each basic unit consists of resistance, inductance, and capacitance. The diagram of the equivalent circuit for the stator coil is shown in Fig. 3 [18].

In Fig. 3, R_s is the equivalent series resistance of the basic unit. Considering the skin effect of the copper conductor and the analyzed frequency band (1 kHz∼10 MHz), the resistance at 1 MHz is calculated, which approximately replaces the variable resistance. It is noted in [18] that the resistance values determined for other frequencies have an insignificant influence on the results. R_i is the electrostatic loss resistance. Leakage inductance L_{s} takes two different values. For the turns located in an end-winding section, the leakage inductance is L_{sa} due to the flux in the air. For the turns found in the slot section, the leakage inductance is L_{ss} due to the flux penetration into the iron core and insulation material between turns and the slot walls. Due to the existence of a magnetic core, L_{ss} is slightly larger than L_{sa}. The inductive coupling between section *i* and *j* is modeled using the mutual inductance defined by $M_{ij} = k\sqrt{L_i L_j}$, *k* is a coefficient depending on the magnetic coupling. It can be chosen between 0.7 and 1 depending on the turn physical closeness in the overhang section [22]. A strong coupling between two adjacent conductors is supposed, in which both the inductive coupling coefficients of L_{sa} and L_{ss} are 0.9 [18]. Besides, the inductive coupling is small and neglected between non-adjacent conductors.

It is noted that the calculations of parameters in Fig. 3 can be found in [18]. The (14) and (15) calculate the L_{ss} and L_{sa},

$$L_{ss} = L_{ss1} + L_{ss2} = \frac{\mu n^2 p}{z} + \frac{\mu_0 n}{2\pi} \ln\left(\frac{2h}{r}\right) \tag{14}$$

$$L_{sa} = \frac{0.112 n^2}{K \ln\left(\frac{2l}{a+b}\right)} \tag{15}$$

The contributions to the coil self-inductance due to the flux penetration into the iron core is L_{ss1}, $p = \sqrt{\rho/jw\mu}$ is the depth of penetration, ρ is the iron resistivity, μ is the iron permeability, *n* is the number of turns in the coil, and *z* is the slot perimeter. L_{ss2} is the inductance due to the flux linking the conductors and the coils in the end winding. μ_0 is the permeability of vacuum, *r* is the equivalent geometric mean radius of conductors, and *h* is half the slot width. L_{sa} is the inductance due to the flux linking the conductors and the coils in the end winding. *K* is the correction factor, *l* is the mean turn's length, *a* and *b* are the turn geometrical dimensions.

C_i is the inter-turn capacitance of the winding. C_m is the grounded capacitance, which represents the coupling relationship between the coil and core. The (16) and (17) calculate the capacitance,

$$C_i = \varepsilon_0 \varepsilon_1 \frac{l_i l}{2e_i} \tag{16}$$

$$C_m = \varepsilon_0 \varepsilon_2 \frac{l_c l}{e_m} \tag{17}$$

Where ε_0 is the vacuum dielectric constant, ε_1 is the relative dielectric constant of the insulation between the winding turns, l_i is the width of the winding conductor, l is the length of the basic unit of the winding, e_i is the thickness of insulation layer, ε_2 is the relative dielectric constant of insulation layer for the winding to the core, e_m is the thickness of insulation layer for the winding to the core, and l_c is the width of the winding conductor.

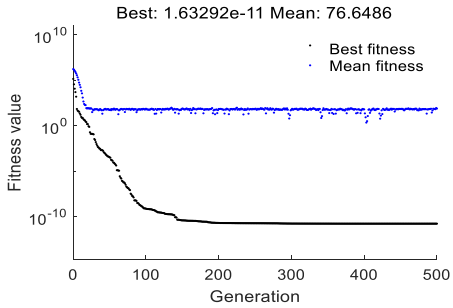

(a)

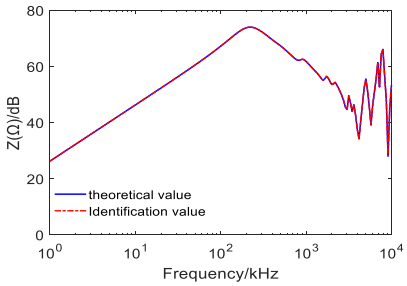

(b)

Fig. 4. Identification result of equivalent circuit parameters for stator coil of simulated AC machine. (a) fitness curve. (b) broadband impedance curves based on identified parameters and actual values.

B. Parameter Identification Results

The equivalent lumped parameter circuit of Fig. 3 is built-in circuit simulation software. The AC sweeping frequency analysis is conducted. The terminal broadband impedance curve is simulated and obtained. Afterward, the circuit parameters are searched based on the proposed method in MATLAB. The circuit parameters to be identified include $R_s, R_i, L_{sa}, L_{ss}, C_i$ and C_m. A server is used for calculation (Intel Xeon Gold 6268*2, 128G RAM, 96 threads). To prevent the parameter search from falling into local optimum, the upper and lower bounds of parameters are restricted to a specific range before identification. The searching for solutions will be more efficient. Besides, the server's parallel computing is used in the parameter identification to improve the convergence speed. The initial population number optimized by GA is set to 600, the population type is set to double-precision vector, random uniform distribution, and the number of iterations is set to 500.

Fig. 4 is the parameter identification result of an equivalent broadband circuit for the simulated AC machine's stator coil. Fig. 4(a) is the fitness curve. The fitness tends to be stable in the latter process of GA optimization algorithm. Fig. 4(b) compares broadband impedance curves based on identified parameters and actual values. The two curves are in good agreement, with a correlation coefficient of 0.99. Table I shows the equivalent circuit's identified and exact parameters for the stator coil of simulated AC machine, respectively, and the relative error is within 2%. The impedance curve of the stator coil is obtained from the simulation. Thus, this section is the verification of the proposed method from the perspective of simulation. The results preliminarily indicate the feasibility of the proposed modeling method.

TABLE I
COMPARISON OF EQUIVALENT CIRCUIT PARAMETERS FOR STATOR COIL OF SIMULATED AC MACHINE

	Actual value	Identification value	Error
R_s/mΩ	0.73	0.72463	-0.74%
R_i/kΩ	1.8	1.83	1.67%
L_{sa}/μH	8	8	0
L_{ss}/μH	10	10	0
C_i/pF	380	380	0
C_m/pF	1.87	1.87	0

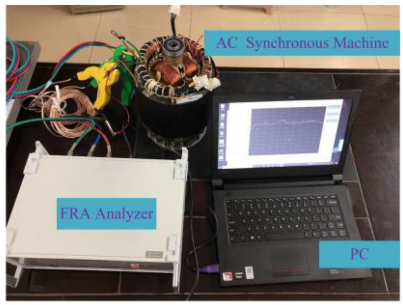

Fig. 5. Image of experimental field test.

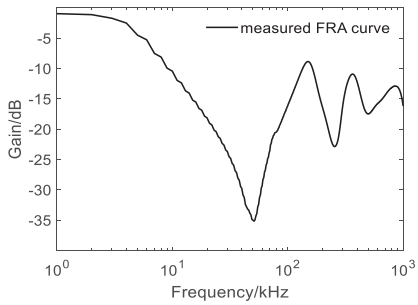

Fig. 6. Frequency response curve of stator winding of 5 kW synchronous machine.

IV. EXPERIMENTAL VERIFICATION OF MODELING BROADBAND EQUIVALENT CIRCUIT FOR STATOR WINDING OF SYNCHRONOUS MACHINE

A. Test Settings and Results

The stator of a 5 kW, 380V, 9.5A, 1500 r.p.m three-phase salient pole synchronous machine is tested to validate the proposed method further. The FRA analyzer (SFRB-R, sweeping frequency accuracy <0.01%, amplitude measurement accuracy $<\pm$1dB) is used to measure the FRA curves of the three-phase stator winding. A sinusoidal sweep signal with the frequency of 1 kHz$\sim$1 MHz and amplitude of 10 V is injected to the neutral point of the stator winding, and the response signal is measured at the terminal of phase winding. The image of the experimental field test is shown in Fig. 5.

Fig. 6 shows the measured FRA curve of the stator U-phase winding of the synchronous machine. There exist three resonant points in the frequency range from 1 kHz to 1 MHz. In the low-frequency band, the effect of winding inductance is much more significant than that of capacitance. Thus, the frequency response curve shows a downward trend. In the high-frequency band, the effect of winding capacitance is much more significant

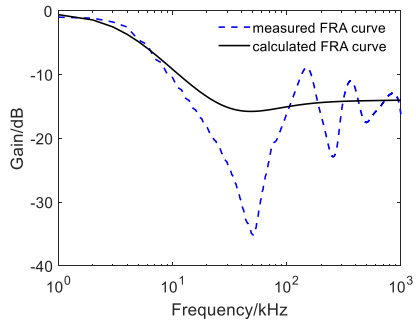

Fig. 7. Parameter identification result when the corresponding parameters of different units are equal.

than that of inductance. Besides, when GA is used to identify the equivalent circuit parameters, the order of magnitude of equivalent parameters can be set in advance to reduce the burden of the algorithm. Refer to [7]–[8], [15], [21], [23], the order of magnitude of C, K, R, G_g, G_s, and L of Fig. 1 can be selected as pF, pF, Ω, kS, kS, and mH. Proper orders of magnitude of electrical parameters reduce the solution's search time and increase the ability to identify parameters to prevent optimization from falling into the local optimum.

B. Parameters Identification Results for the Situation that the Corresponding Parameters of Different Units are Equal

Firstly, the situation that the corresponding parameters of different units of Fig. 1 are equal is considered (namely, the related parameters of R, L, C, K and G in other units are identical). In this optimization problem, a linear constraint is introduced to reduce the analytic space to speed up the convergence, including equality and inequality constraints. In the equality constraints, the C, K, R_s and L_s of each unit are equal. In inequality constraints, mutual inductance is smaller than self-inductance. Inequality constraints are shown in (18).

$$L_{ii} > M_{ij}, L_{jj} > M_{ij} (i \neq j) \tag{18}$$

Reference [24] shows that the equivalent units' order can be determined by the number of resonance peaks in the frequency response curve. As proposed, the order of the equivalent units is selected as 3 in this section. Fig. 7 shows the result of parameter identification when the corresponding parameters of different units are equal. The results of related parameter identification are given in Table II. It is noted that the calculated parameters are frequency-independent in the state-space model. By comparing with the measured FRA curves, there is a significant deviation in the parameter identification results. The computed curve only has the same trend as the measured one in the low-frequency band. It is unacceptable for parameter identification results after 30 kHz. The information of entire resonances and anti-resonance is lost.

TABLE II
IDENTIFICATION RESULTS OF EQUIVALENT CIRCUIT PARAMETERS OF STATOR U-PHASE WINDING

parameter	value	parameter	value
R_{s1}	0.533963 $m\Omega$	M_{23}	0.383028 μH
R_{s2}	0.533963 $m\Omega$	C_1	22.9418 nF
R_{s3}	0.533963 $m\Omega$	C_2	22.9418 nF
L_{11}	0.0474388 mH	C_3	22.9418 nF
L_{22}	0.0474388 mH	C_4	22.9418 nF
L_{33}	0.0474388 mH	K_1	3.86068 nF
M_{12}	0.682997 μH	K_2	3.86068 nF
M_{13}	0.055659 μH	K_3	3.86068 nF

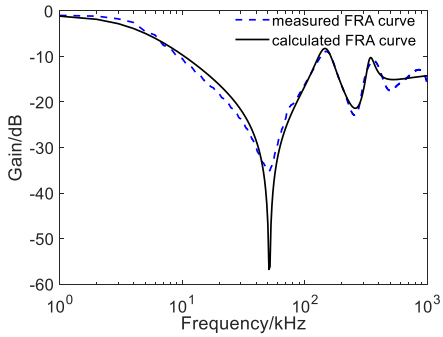

Fig. 8. Parameter identification result when the corresponding parameters of each unit are unequal.

C. Parameters Identification Results for the Situation that the Corresponding Parameters of Different Units are Unequal

The layout and structure of windings for different slots are slightly different; we considered that the corresponding parameters of various units of Fig. 1 are unequal. This study aims to find a simple method to cover resonance points in the FRA, which can predict the winding behavior with acceptable accuracy and by using the minimum number of units. Each unit of the equivalent circuit corresponds to a certain length and a certain number of turns [24]. In this subsection's optimization problem, the introduced linear constraint is only the inequality constraint of (18).

Fig. 8 shows the result of parameter identification when the corresponding parameters of each unit of the equivalent circuit model are unequal. The results of related parameter identification are given in Table III. The identified parameters are also frequency independent. The calculated FRA curve based on the parameter identification result is in agreement with the measured FRA curve. Due to simplifications in establishing the model, for instance, neglecting the conductance parameters, there is a difference in the amplitude at the first resonance point. However, the frequencies and amplitudes of other resonance and anti-resonance are identical. The two FRA curves have the same trend, which again demonstrates the proposed modeling method's feasibility. It also should be noted that both the electrical machinery and electrical model are different for

TABLE III
IDENTIFICATION RESULTS OF EQUIVALENT CIRCUIT PARAMETERS OF STATOR U-PHASE WINDING

parameter	value	parameter	value
R_{s1}	4.11252 $m\Omega$	M_{23}	0.0264791 mH
R_{s2}	6.27517 $\mu\Omega$	C_1	6.30636 nF
R_{s3}	5.35873 Ω	C_2	3.71574×10^{-6} nF
L_{11}	0.0594174 mH	C_3	9.56255 nF
L_{22}	1.89469 mH	C_4	0.515412 nF
L_{33}	0.030272 mH	K_1	6.13099 nF
M_{12}	0.0584397 mH	K_2	5.18056 nF
M_{13}	0.0239343 mH	K_3	12.7793 nF

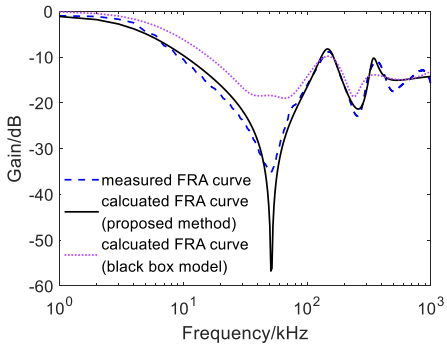

Fig. 9. Comparison of FRA curves calculated by different methods.

simulation and experiment. The FRA curve of Fig. 8 is different from that of Fig. 4. Finally, comparing the results of Fig. 7 and Fig. 8, it is more practical to use the precondition that each unit of the equivalent circuit model's corresponding parameters is unequal before performing modeling. The result of parameter identification is more accurate.

D. Comparison With the Existing Black-Box Model

As mentioned before, the modeling process of small and medium rated power synchronous machines using the white-box method is challenging to achieve, and the results are not acceptable. Therefore, the comparison of modeling methods is conducted between the proposed method and the black-box model. A black-box model is constructed according to [19]. The model is built based on the number of peaks and valleys of the entire terminal broadband characteristics, and each essential section is composed of a parallel RLC resonant unit.

The comparison of FRA curves calculated by different methods is shown in Fig. 9. It can be seen that the FRA curve based on the black-box model can only roughly reflect the position of the resonance point, and there are two resonant points around 30∼60 kHz. Besides, large deviations exist in the amplitude between the calculated FRA curve based on the black box model and the measured FRA curve. Compared with the gray box model, the black-box model is not suitable for this machine.

In short, the proposed method has some benefits as follows.

1) Time is not a concern, as time is not essential when the objective is modeling; only one modeling process of the synchronous machine is required. Thus, although the computer used for modeling in this study is powerful, a general computer is still usable.
2) This method is simpler than other methods, for instance, the white box model, which requires extensive calculations. It can also provide better matching with measurement results.
3) The equivalent electrical parameters can be automatically extracted even if no detailed geometrical and physical information of machine winding is available.
4) This method uses the equivalent electrical circuit with the minimum number of units to cover most resonance points in the FRA, which can predict the winding behavior with acceptable accuracy.
5) The electrical model established by this method can simulate and analyze the machine's winding faults for frequency response analysis.

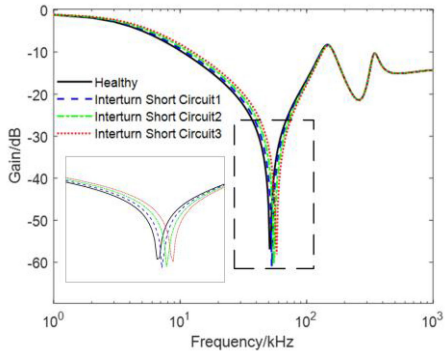

Fig. 10. Simulation results of stator winding inter-turn short circuit fault of synchronous machine.

V. DIAGNOSTIC ANALYSIS OF STATOR WINDING INTER-TURN SHORT CIRCUIT FAULT OF SYNCHRONOUS MACHINE

In this section, the established broadband equivalent circuit model of the above 5 kW machine in the previous section is used to simulate the inter-turn short-circuit fault. The inter-turn short circuit fault of windings can cause the change of equivalent inductance parameters [23]. The extent of the inter-turn short-circuits fault is simulated by setting different inductance of basic unit in the equivalent circuit model [4]. The simulated end-to-end open circuit FRA curve is shown in Fig. 10. In Fig. 10, the numbers after the term "Interturn Short Circuit" indicate the fault degree of inter-turn short-circuit fault, and the fault degree "1" is smaller than fault degree "2", and so on. The term "1", "2" and "3" indicate the corresponding inductances are 94%, 87%, and 81% of the inductance in the health status, respectively.

To validate the simulation result of Fig. 10, the actual machine's inter-turn short-circuit fault is made by stripping the external insulating paint of the stator winding and shortening the adjacent turns. The experiment wiring of the FRA analyzer and machine is shown in Fig. 11. We named the short circuit points terminal 1, 2, and 3. Thus, the short circuit fault extent is realized by shortening different terminals. Fig. 12 shows the measured FRA curves of the stator winding inter-turn short circuit fault.

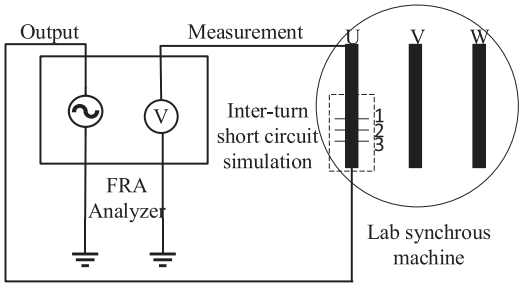

Fig. 11. Experiment diagram of inter-turn short circuit fault of phase-U winding.

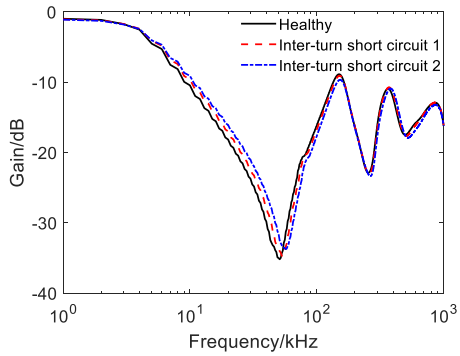

Fig. 12. Measurement results of the stator winding inter-turn short circuit fault.

The changing trend of measured FRA curves is similar to that of simulated curves shown in Fig. 10. Besides, Fig. 10 is also similar to that of the measured FRA curve of the stator winding inter-turn short circuit fault of a large 40 MVA synchronous machine pole in [23], which once again demonstrates the correctness of the proposed broadband equivalent circuit model.

According to Fig. 10, the stator winding's FRA curve is changed due to the inter-turn short circuit fault, and the anti-resonances of the FRA curve are shifted to the high-frequency band compared with the healthy signature. With the increase of fault degree, the variations of anti-resonance are more significant. To carry out the quantitative analysis of variable FRA curves, we refer to the Chinese power industry standard DL/T 911, which is used for frequency response analysis of power transformers. The evaluating mathematical indicator-relative factor (R_{XY}) is used. The formula for calculating R_{XY} [25] is shown in (19)

$$R_{XY} = \begin{cases} 10 & 1 - P_{XY} < 10 \\ -\log_{10}(1 - P_{XY}) & \text{otherwise} \end{cases} \tag{19}$$

where P_{XY} is given by

$$P_{XY} = \frac{\frac{1}{N}\sum_{i=1}^{N}\left(X_i - \frac{1}{N}\sum_{i=1}^{N} X_i\right)^2\left(Y_i - \frac{1}{N}\sum_{i=1}^{N} Y_i\right)^2}{\sqrt{D_X D_Y}} \tag{20}$$

$$D_X = \frac{1}{N}\sum_{i=1}^{N}\left(X_i - \sum_{i=1}^{N} X_i\right)^2 \tag{21}$$

TABLE IV
DEFORMATION LEVELS AND THE CORRESPONDING RELATIVE FACTOR VALUES AT LOW(LF), MEDIUM(MF) AND HIGH(HF) FREQUENCIES

Deformation level	Limits for R_{XY}
Severe	R_{LF}<0.6
Moderate	1.0>R_{LF}≥0.6 or R_{MF}<0.6
Slight	2.0>R_{LF}≥1.0 or 0.6≤R_{MF}<1
Normal winding	R_{LF}≥2.0,R_{MF}≥1.0,and R_{HF}≥0.6
LF:1 kHz to 100kHz,MF:100kHz to 600kHz,HF:600kHz to 1MHz	

TABLE V
COMPARISON OF MATHEMATICAL INDICATOR FOR SIMULATED FRA CURVES

Failure Condition	Correlation Coefficient		
	1~100 kHz	100~600 kHz	600~1000 kHz
Inter-turn Short Circuit 1	1.4439	3.7237	9.5682
Inter-turn Short Circuit 2	1.0281	3.0512	9.4933
Inter-turn Short Circuit 3	0.8034	2.6221	8.9089

TABLE VI
CHARACTERISTIC POINT INFORMATION OF FREQUENCY RESPONSE SIGNATURES OF INTER-TURN SHORT CIRCUIT FAULT

Failure Condition	Feature Point Information	
	Frequency/kHz	Change Rate
Healthy	51	/
Inter-turn Short Circuit 1	53	3.92%
Inter-turn Short Circuit 2	55	7.84%
Inter-turn Short Circuit 3	58	13.73%

$$D_Y = \frac{1}{N}\sum_{i=1}^{N}\left(Y_i - \frac{1}{N}\sum_{i=1}^{N} Y_i\right)^2 \tag{22}$$

Where X_i and Y_i are the *i*th elements of the fingerprint and measured FRA traces, respectively, and N is the number of elements.

Table IV shows the evaluation criteria of a relative factor in DL/T 911, in which the status of winding can be diagnosed as normal, slight, moderate, and severe. The entire frequency band of the FRA curve is divided into three bands: low frequency (1∼100 kHz), medium frequency (100∼600 kHz), and high frequency (600∼1000 kHz). Table V shows calculated R_{XY} for FRA curves of Fig. 10. The relative factor of each sub-frequency band decreases with the increase of fault degree. There exist few reports regarding the application of relative factor to diagnose the winding faults of electrical machinery. This study still refers to the Chinese standard DL/T 911, the inter-turn short circuit 1 and 2 are interpreted as slight deformation, and the inter-turn short circuit 3 is diagnosed as moderate deformation.

Besides, the first anti-resonance of the FRA signature can be selected as the feature point based on Fig. 10. Table VI shows the information of the feature point of the FRA curve in Fig. 10. The frequency change rate of the feature point of faulty winding is 3.92%, 7.84%, and 13.73%. The frequency change of the feature point increases with the increase of the fault extent. The

above results demonstrate that the relative factor and feature point information of the FRA curve can be used to diagnose and analyze winding inter-turn short circuit fault.

VI. Conclusion

1) A developing procedure that facilitates broadband equivalent circuit modeling of synchronous machine winding based on the gray-box model has been presented. The model is established using the terminal broadband characteristics of electrical machinery, based on the state-space model and GA optimization. The simulation and experimental results verify the feasibility of the proposed procedure, and the FRA curves corresponding to the parameter identification results are highly coincident with the actual curves.
2) During the identification of equivalent parameters, both cases of equal parameters and unequal parameters of each unit are considered. The results show that it is more practical to use unequal parameters as the premise for modeling, and the consequences of parameter identification are more accurate. The comparison result with existing methods shows the proposed method's superiority over that based on the black box model.
3) In the established equivalent circuit model of 5 kW machine, the winding inter-turn short circuit fault is simulated. The FRA curve of the fault winding changes significantly compared with that of a healthy one, and the inter-turn short circuit causes the deviation of the FRA curve to the high-frequency band.
4) The FRA curve's first resonant point is selected as the feature point for fault analysis. Its frequency information can be used to diagnose the inter-turn short circuit fault effectively. The experimental results also indicate the feasibility of using FRA to detect a synchronous machine's winding fault.
5) The automatic parameter extraction makes the modeling process easy to implement. The proposed model can also simulate the machine's internal winding faults for frequency response analysis. However, the method and conclusions are suitable for the machine introduced in this study. The applicability to the synchronous machine of other specifications needs to be further studied in the future.

Acknowledgment

It will also contain support information, including sponsor and financial support acknowledgment.

References

[1] K. Shi, W. Song, H. Ge, P. Xu, Y. Yang, and F. Blaabjerg, "Transient analysis of microgrids with parallel synchronous generators and virtual synchronous generators," *IEEE Trans. Energy Convers.*, vol. 35, no. 1, pp. 95–105, Mar. 2020.

[2] H. Henao *et al.*, "Trends in fault diagnosis for electrical machines: A review of diagnostic techniques," *IEEE Ind. Electron.*, vol. 8, no. 2, pp. 31–42, Jun. 2014.

[3] Y. B. Shao, "Fault analysis and processing for large generator stator winding," *Large Electric Mach. Hydraulic Turbine*, vol. 2014, no. 6, pp. 27–31, Nov. 2014.

[4] Z. D. Jia, H. Lu, and Z. P. Zhang, "Modeling simulation and diagnosis analysis of inter-turn short circuits fault in generator rotor," *High Voltage Eng.*, vol. 45, no. 12, pp. 3932–3940, 2019.

[5] T. Li, "Simulation study on interturn short circuit of rotor windings in generator by RSO method," in *Proc. Int. Conf. High Voltage Eng. Appl.*, ATHENS, Greece, 2018, pp. 1–4.

[6] G. Capolino and A. Cavagnino, "New trends in electrical machines technology—Part II," *IEEE Trans. Ind. Electron.*, vol. 61, no. 9, pp. 4931–4936, Sep. 2014.

[7] F. R. Blánquez, C. A. Platero, E. Rebollo, and F. Blánquez, "Evaluation of the applicability of FRA for inter-turn fault detection in stator windings," in *Proc. 9th IEEE Int. Symp. Diagnostics Electric Mach., Power Electron. Drives*, Valencia, 2013, pp. 177–182.

[8] F. R. Blánquez, C. A. Platero, E. Rebollo, and F. Blázquez, "Field-winding fault detection in synchronous machines with static excitation through frequency response analysis," *Int. J. Elect. Power Energy Syst.*, vol. 73, pp. 229–239, 2015.

[9] C. A. P. Gaona, F. Blázquez, P. Frías, and M. Redondo, "A novel rotor ground-fault-detection technique for synchronous machines with static excitation," *IEEE Trans. Energy Convers.*, vol. 25, no. 4, pp. 965–973, Dec. 2010.

[10] C. A. Platero, F. Blázquez, P. Frías, and M. Pardo, "New on-line rotor ground fault location method for synchronous machines with static excitation," *IEEE Trans. Energy Convers.*, vol. 26, no. 2, pp. 572–580, Jun. 2011.

[11] S. Wang, S. Wang, H. Feng, Z. Guo, S. Wang, and H. Li, "A new interpretation of FRA results by sensitivity analysis method of two FRA measurement connection ways," *IEEE Trans. Magn.*, vol. 54, no. 3, Mar. 2018, Art. no. 8400204.

[12] V. Nurmanova, M. Bagheri, A. Zollanvari, K. Aliakhmet, Y. Akhmetov, and G. B. Gharehpetian, "A new transformer FRA measurement technique to reach smart interpretation for inter-disk faults," *IEEE Trans. Power Del.*, vol. 34, no. 4, pp. 1508–1519, Aug. 2019.

[13] X. Mao, Z. Wang, Z. Wang, and P. Jarman, "Accurate estimating algorithm of transfer function for transformer FRA diagnosis," in *Proc. IEEE Power Energy Soc. General Meet.*, Portland, OR, USA, 2018, pp. 1–5.

[14] N. Hashemnia, A. Abu-Siada, and S. Islam, "Improved power transformer winding fault detection using FRA diagnostics – Part 1: Axial displacement simulation," *IEEE Trans. Dielectr. Electr. Insul.*, vol. 22, no. 1, pp. 556–563, Feb. 2015.

[15] Z. Zhao, C. Yao, C. Li, and S. Islam, "Detection of power transformer winding deformation using improved fra based on binary morphology and extreme point variation," *IEEE Trans. Ind. Electron.*, vol. 65, no. 4, pp. 3509–3519, Apr. 2018.

[16] J. Liu, Z. Zhao, and C. Tang, "Classifying transformer winding deformation fault types and degrees using FRA based on support vector machine," *IEEE Access,* vol. 7, pp. 112494–112504, 2019.

[17] O. A. Mohammed, S. Ganu, N. Abed, S. Liu, and Z. Liu, "High frequency PM synchronous motor model determined by FE analysis," *IEEE Trans. Magn.*, vol. 42, no. 4, pp. 1291–1294, Apr. 2006.

[18] F. Perisse, P. Werynski, and D. Roger, "A new method for AC machine turn insulation diagnostic based on high frequency resonances," *IEEE Trans. Dielectr. Electr. Insul.*, vol. 14, no. 5, pp. 1308–1315, Oct. 2007.

[19] Q. D. Wang, H. Sun, and Y. L. Liu,"Fast modeling of the motor broadband equivalent circuit model," *J. Chongqing Univ.*, vol. 35, no. 12, pp. 34–39, 2012.

[20] N. Idir, Y. Weens, M. Moreau, and J. J. Franchaud, "High-frequency behavior models of AC motors," *IEEE Trans. Magn.*, vol. 45, no. 1, pp. 133–138, Jan. 2009.

[21] L. Wang, C. Ngai-Man Ho, F. Canales, and J. Jatskevich, "High-frequency modeling of the long-cable-fed induction motor drive system using TLM approach for predicting overvoltage transients," *IEEE Trans Power Electr,* vol. 25, no. 10, pp. 2653–2664, Oct. 2010.

[22] J. M. M. Tarifa, H. A. Duarte, and J. S. Feito, "Characterization of turn to turn insulation electrical stresses in random wound coils at high frequencies," in *Proc. IEEE Int. Conf. Solid Dielectrics*, Toulouse, France, 2004, vol. 2, pp. 884–887.

[23] A. Mugarra, C. A. Platero, J. A. Martínez, and U. Albizuri-Txurruka, "Validity of frequency response analysis (FRA) for diagnosing large salient poles of synchronouos machines," *IEEE Trans. Ind. Appl.*, vol. 56, no. 1, pp. 226–234, Jan./ Feb. 2020.

[24] M. M. Shabestary, A. J. Ghanizadeh, G. B. Gharehpetian, and M. Agha-Mirsalim, "Ladder network parameters determination considering non-dominant resonances of the transformer winding," *IEEE Trans. Power Del.*, vol. 29, no. 1, pp. 108–117, Feb. 2014.
[25] M. Bagheri, M. S. Naderi, T. Blackburn, and T. Phung, "Frequency response analysis and short-circuit impedance measurement in detection of winding deformation within power transformers," *IEEE Electr. Insul. Mag.*, vol. 29, no. 3, pp. 33–40, Jun. 2013.

Zhongyong Zhao (Member, IEEE) was born in Guangyuan, China. He received the B.S. and Ph.D. degrees in electrical engineering from Chongqing University, Chongqing, China, in 2011 and 2017, respectively. He is currently an Associate Professor with the College of Engineering and Technology, Southwest University, Chongqing, China. His research interests include condition monitoring and fault diagnosing for HV apparatus, and artificial intelligence. He was the recipient the Scholarship from China Scholarship Council to enable him to attend a joint-training Ph.D. program with Curtin University, Perth, WA, Australia, from 2015 to 2016.

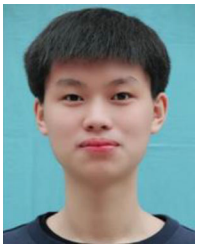

Yu Chen was born in Wenzhou, China, in 2000. He is currently working toward the bachelor's degree with the Department of Electrical Engineering, College of Engineering and Technology, Southwest University, Chongqing, China. His research interests include condition monitoring and fault diagnosing for power transformer, and application of artificial intelligence.

Yueqiang Yu was born in Nanchong, China, in 1994. He is currently working toward the master's degree with the Department of Electrical Engineering, College of Engineering and Technology, Southwest University, Chongqing, China. His research interests include condition monitoring and fault diagnosing for synchronous machine.

Mengyuan Han was born in Dezhou, China, in 1996. She is currently working toward the master's degree with the Department of Electrical Engineering, College of Engineering and Technology, Southwest University, Chongqing, China. Her research interests include condition monitoring and fault diagnosing for electric machinery, and application of artificial.

Chao Tang (Member, IEEE) was born in Sichuan, China, in 1981. He received the M.S. and Ph.D. degrees in electrical engineering from Chongqing University, Chongqing, China, in 2007 and 2010, respectively. From 2008 to 2009, he was a Ph.D. Student, and in 2013 and from 2015 to 2016, a Visiting Scholar with the Tony Davies High Voltage Laboratory, University of Southampton, Southampton, U.K., doing research on the dielectric response characteristics and space charge behaviors of oil-paper insulation. He is currently a Professor with the College of Engineering Technology, Southwest University, Chongqing, China. His research interests include mainly in the aging of online monitoring of insulation conditions and fault diagnosis for high-voltage equipment.

Chenguo Yao (Member, IEEE) was born in Nanchong, China. He received the B.S., M.S., and Ph.D. degrees in electrical engineering from Chongqing University, Chongqing, China, in 1997, 2000, and 2003, respectively. In 2007, he became a Professor with the School of Electrical Engineering, Chongqing University. From 2017 to 2018, he was a Visiting Scholar with Old Dominion University, Norfolk, VA, USA. His current works include online monitoring of insulation condition and insulation fault diagnosis for HV apparatus, pulsed power technology, and its application in biomedical engineering.